ARTICLE

BIOTECHNOLOGY and BIOENGINEERING

A Versatile Coupled Cell-Free Transcription–Translation System Based on Tobacco BY-2 Cell Lysates

Matthias Buntru, Simon Vogel, Katrin Stoff, Holger Spiegel, Stefan Schillberg

Fraunhofer Institute for Molecular Biology and Applied Ecology IME, Forckenbeckstrasse 6, Aachen 52074, Germany; telephone: 49–241-6085–11050; fax: 49–241-6085–10000; e-mail: stefan.schillberg@ime.fraunhofer.de

ABSTRACT: Cell-free protein synthesis is a powerful method for the high-throughput production of recombinant proteins, especially proteins that are difficult to express in living cells. Here we describe a coupled cell-free transcription–translation system based on tobacco BY-2 cell lysates (BYLs). Using a combination of fractional factorial designs and response surface models, we developed a cap-independent system that produces more than 250 μg/mL of functional enhanced yellow fluorescent protein (eYFP) and about 270 μg/mL of firefly luciferase using plasmid templates, and up to 180 μg/mL eYFP using linear templates (PCR products) in 18 h batch reactions. The BYL contains actively-translocating microsomal vesicles derived from the endoplasmic reticulum, promoting the formation of disulfide bonds, glycosylation and the cotranslational integration of membrane proteins. This was demonstrated by expressing a functional full-size antibody (~150 μg/mL), the model enzyme glucose oxidase (GOx) (~7.3 U/mL), and a transmembrane growth factor (~25 μg/mL). Subsequent in vitro treatment of GOx with peptide-N-glycosidase F confirmed the presence of N-glycans. Our results show that the BYL can be used as a high-throughput expression and screening platform that is particularly suitable for complex and cytotoxic proteins.

Biotechnol. Bioeng. 2015;112: 867–878.

KEYWORDS: BY-2 cell lysate; cell-free protein synthesis; coupled transcription–translation; high-throughput screening; protein expression

Introduction

The increasing demand for new therapeutic proteins, technical enzymes, protein engineering, and functional genomics requires a rapid and efficient protein production and screening platform (Leader et al., 2008; Swartz, 2012). The emerging technology of cell-free protein synthesis (CFPS) can help to satisfy this demand (Carlson et al., 20125). Compared to cell-based expression, CFPS offers advantages such as shorter process times and the direct control and monitoring of reaction conditions (Swartz, 2012). PCR products can be used directly for the simultaneous expression of multiple proteins without laborious cloning and transformation steps (Gan and Jewett, 2014; Yabuki et al., 2007; Wu et al., 2007a). CFPS platforms allow the addition of accessory factors that promote protein folding (Endo et al., 2006; Matsuda et al., 2006; Ozawa et al., 2005) or the incorporation of unnatural amino acids (Albayrak and Swartz, 2013; White et al., 2013). They also facilitate the expression of cytotoxic proteins that cannot be produced in living cells (Schwarz et al., 2008; Xu et al., 2005; Xun et al., 2009).

Escherichia coli cell-free lysates are widely used and are advantageous because of their low cost, scalability and high productivity (Caschera and Noireaux, 2014; Zawada et al., 2011). However, because the lysates originate from bacteria, they are unsuitable for the production of complex proteins with multiple subdomains due to inefficient oxidative folding and the absence of chaperones and glycosylation machinery. Eukaryotic cell-free systems are better suited for the expression of such proteins and support most forms of post-translational modification (Chang et al., 2005; Zhang and Kaufman, 2006). The most frequently used systems are based on wheat germ extract (WGE), insect cell extract (ICE) and rabbit reticulocyte lysate (RLL). However, these systems are expensive and extract preparation is complex (Carlson et al., 2012). This has created a demand for additional eukaryotic CFPS such as those based on *Leishmania tarentolae* (Mureev et al., 2009), Chinese hamster ovary (CHO) cells (Brodel et al., 2014) and

Conflicts of interest: None

Abbreviations: ABTS, 2,2′-azino-bis-(3-ethylbenzthiazoline-6-sulfonic acid); AP, alkaline phosphatase; BYL, BY-2 lysate; CECF, continuous-exchange cell-free; CFPS, cell-free protein synthesis; CHO, Chinese hamster ovary; DDM, n-dodecyl-β-D-maltopyranoside; DoE, design of experiments; ER, endoplasmic reticulum; eYFP, enhanced yellow fluorescent protein; Fab, fragment antigen-binding; FFLuc, firefly luciferase; GOx, glucose oxidase; HbEGF, heparin-binding EGF-like growth factor; HC, heavy chain; HRP, horseradish peroxidase; ICE, insect cell extract; IMAC, immobilized metal-affinity chromatography; LC, light chain; MSP, melittin signal peptide; PNGase F, peptide-N-glycosidase F; RLL, rabbit reticulocyte lysate; scFv, single-chain variable fragment; SEC, size exclusion chromatography; TMV, *Tobacco mosaic virus*; UTR, untranslated region; WGE, wheat germ extract.

Correspondence to: Stefan Schillberg

Contract grant sponsor: Federal Ministry of Education and Research
Contract grant number: BMBF, FKZ 0315942
Contract grant sponsor: Fraunhofer Society
Received 9 September 2014; Accepted 17 November 2014
Accepted manuscript online 25 November 2014;
Article first published online 16 January 2015 in Wiley Online Library (http://onlinelibrary.wiley.com/doi/10.1002/bit.25502/abstract).
DOI 10.1002/bit.25502

Saccharomyces cerevisiae (Gan and Jewett, 2014; Hodgman and Jewett, 2013).

An uncoupled CFPS system based on tobacco BY-2 cells has been reported before (Buntru et al., 2014 ; Gursinsky et al., 2009; Komoda et al., 2004). However, we have developed an alternative coupled transcription–translation system based on our previously described BY-2 lysate (BYL), which can be prepared in large amounts from inexpensive cell cultures grown under controlled conditions in less than 1 day (Buntru et al., 2014). The reaction conditions were optimized using a design of experiments (DoE) approach to quantify interdependent variables and their interactions (Jewett and Swartz, 2004). Statistically designed experiments varying several factors simultaneously are more efficient than testing one factor at a time (Wu et al., 2007b). DoE strategies require fewer resources (in terms of experiments, time and raw materials), the effects of each factor are determined more accurately, the interactions among factors can be predicted systematically, and the experimental data cover a larger region of the design space (Czitrom, 1999; Vaidya et al., 2009).

Our novel BYL system was tested against a commercial WGE for the production of the reporter proteins enhanced yellow fluorescent protein (eYFP) and firefly luciferase (FFLuc). The ability of the BYL system to promote oxidative folding, post-translational modification, and the assembly of multi-domain proteins was evaluated by the expression of a homodimeric glycoprotein enzyme and a heterotetrameric full-size antibody. We also compared the use of plasmid versus linear templates and tested the expression of an integral membrane protein.

Materials and Methods

Plant Material

Tobacco cells (*Nicotiana tabacum* L. cv. Bright Yellow 2, BY-2) were cultivated continuously in a 5-L fermenter (Type 100e, Applicon Biotechnology, AC Schiedam, Netherlands) while maintaining a packed cell volume of 20% at 26°C in the dark. We used Murashige-Skoog liquid medium (Murashige and Skoog basal salt mixture, Duchefa Biochemie, Haarlem, Netherlands) supplemented with 3% (w/v) sucrose, 1 mg/L thiamine-HCl, 0.2 mg/L 2,4 dichlorophenoxyacetic acid, 100 mg/L myo-inositol, 250 mg/L potassium dihydrogen orthophosphate, and Pluronic L-61 antifoam (BASF, Mount Olive, NJ).

Preparation of the BY-2 Cell Lysate

The BYL was prepared as described previously (Buntru et al., 2014) with some modifications. BY-2 cells were harvested during the exponential growth phase of a continuous fermentation at a constant packed cell volume of 20%. They were treated with 3% (v/v) Rohament CL and 0.2% (v/v) Rohapect UF (AB Enzymes, Darmstadt, Germany) in 3.6 g/L Kao and Michayluk basal salts (Duchefa Biochemie), 360 mM mannitol, 1 mg/L 6-benzylaminopurine (BAP) (Sigma-Aldrich, Seelze, Hannover, Germany) and 0.5 mg/L 1-naphtylacetic acid (NAA) (Sigma-Aldrich). The resulting protoplasts were layered onto a discontinuous Percoll gradient containing (from bottom to top) 70% (v/v, 3 mL), 40% (v/v, 5 mL), 30% (v/v, 3 mL), 15% (v/v, 3 mL), and 0% (3 mL) Percoll (GE Healthcare, Munich, Germany) in 0.7 M mannitol, 20 mM $MgCl_2$ and 5 mM PIPES-KOH (pH 7.0) in a 50 mL polypropylene tube (Greiner Bio-One, Frickenhausen, Germany). After centrifugation at 6800 × *g* for 1 h at 25°C in a swinging-bucket rotor (JS-5.3, Beckmann-Coulter, Krefeld, Germany), evacuolated protoplasts were recovered from the 40–70% (v/v) Percoll solution interface and suspended in 3–3.5 volumes of TR buffer (30 mM HEPES-KOH (pH 7.4), 60 mM potassium glutamate, 0.5 mM magnesium glutamate, 2 mM DTT) supplemented with one tablet per 50 mL of Complete EDTA-free Protease Inhibitor Mixture (Roche Diagnostics, Mannheim, Germany). The protoplasts were disrupted on ice using 15 strokes of a Dounce homogenizer (Braun, Melsungen, Germany), and the nuclei and non-disrupted cells were removed by centrifugation at 500 × *g* for 10 min at 4°C. The supernatant was supplemented with 0.5 mM $CaCl_2$ and treated with 7.5 U/mL nuclease S7 (Roche Diagnostics) for 15 min at 20°C. The lysate was supplemented with 2 mM EGTA to inactivate the nuclease by chelating Ca^{2+} and was then frozen in 1 mL aliquots at −80°C. The protein concentration of the final lysate was determined using a colorimetric assay (Bradford, 1976).

Plasmid Constructs

Vector pIVEX_GAA_Omega_eYFP-His was prepared by inserting annealed oligonucleotides 1 and 2 (Table S1) containing the T7 promoter and the *Tobacco mosaic virus* 5′ omega leader sequence with GAA as the first nucleotide triplet into pIVEX1.3_eYFP-His (kindly provided by Dr. Stefan Kubick, Fraunhofer Institute for Cell Therapy and Immunology IZI, Potsdam-Golm, Germany) using the NspI and NcoI sites. Vector pIVEX_GAA_Omega_FFLuc-His was prepared by introducing the FFLuc-His sequence from pIVEX1.3_FFLuc-His (Buntru et al., 2014) into pIVEX_GAA_Omega_eYFP-His using the NcoI and KpnI sites. For vector pIVEX_GAA_Omega_Strep-eYFP containing an N-terminal streptavidin affinity tag, the Strep-eYFP sequence was amplified by PCR using pIX3.0_Strep-eYFP as a template (kindly provided by Dr. Stefan Kubick) with primers 3 and 4 (Table S1). The PCR product was digested with PciI and Acc65I and inserted into the NcoI and Acc65I sites of pIVEX_GAA_Omega_eYFP-His. Vector pF3A_WG_eYFP-His was prepared by transferring the eYFP-His sequence from pIVEX_GAA_Omega_eYFP-His into pF3A_WG (Promega, Mannheim, Germany) using the NcoI and KpnI sites. Vector pIVEX_GAA_Omega_MSP-eYFP-His was prepared by inserting annealed oligonucleotides 5 and 6 (Table S1) containing the melittin signal peptide (MSP) sequence from *Apis mellifera* into pIVEX_GAA_Omega_eYFP-His using the NcoI site. Vector pIVEX_GAA_Omega_MSP-HbEGF-eYFP-His was prepared by introducing the HbEGF-eYFP sequence containing a part of the MSP from pIVEX1.3_MSP-HbEGF-eYFP-His (kindly provided by Dr. Stefan Kubick) into pIVEX_GAA_Omega_MSP-eYFP-His using the AccI and XmaI sites. For vector pIVEX_GAA_Omega_MSP-GOx-His, the GOx sequence was amplified by PCR using pYES2_GOx as the template (kindly provided by Dr. Raluca Ostafe, RWTH Aachen University, Aachen, Germany) with primers 7 and 8 (Table S1). The PCR product was digested with Esp3I and XmaI and inserted into the NcoI and XmaI sites of pIVEX_GAA_Omega_MSP-eYFP-His. For vector pIVEX_GAA_Omega_MSP-M12LC-His, the light chain (LC) sequence from human antibody M12 (Raven et al., 2014) was

amplified by PCR using pTRAkc_MTAD as a template (kindly provided by Dr. Nicole Raven, Fraunhofer IME, Aachen, Germany) with primers 9 and 10 (Table S1). For vector pIVEX_GAA_Omega_MSP-M12HC-His, the heavy chain (HC) sequence from human antibody M12 was amplified by PCR using pTRAkc_MTAD as the template with primers 11 and 12 (Table S1). The resulting PCR products were digested with NcoI and NotI and inserted into the NcoI and NotI sites of pIVEX_GAA_Omega_MSP-eYFP-His. The Strep-eYFP PCR product was amplified by PCR using pIVEX_GAA_Omega_Strep-eYFP as a template with primers 13 and 14 (Table S1). The modified Strep-eYFP PCR product was amplified by PCR using pIVEX_GAA_Omega_Strep-eYFP as the template with phosphorothioate-modified primers 9 and 10.

Coupled Transcription–Translation Cell-Free Protein Synthesis

Coupled transcription–translation reactions were carried out in 50-μL aliquots at 25°C and 700 rpm for 18 h in a thermomixer (Eppendorf, Hamburg, Germany). Standard reactions contained 40% (v/v) BYL, 40 mM HEPES-KOH (pH 7.8), 8.5 mM magnesium glutamate, 3 mM ATP, 1.2 mM GTP, 1.2 mM CTP, 1.2 mM UTP, 30 mM creatine phosphate, 50 μg/mL creatine kinase, 80 ng/μL vector DNA (∼34 nM), and 50 ng/μL in-house T7 RNA polymerase. WGE (TNT® SP6 High-Yield Wheat Germ Protein Expression System, Promega) transcription–translation reactions were carried out according to the manufacturer's instructions.

Design of Experiments

A DoE approach was used to determine the effect of factors and their interactions on the yield of eYFP produced using the BYL system. We used fractional factorial designs and response surface models in Design Expert v8.0 (Stat-Ease Inc., MN). There were seven factors (A–G) included in the model: (A) HEPES-KOH, pH7.8; (B) magnesium glutamate; (C) potassium glutamate; (D) NTPs; (E) creatine phosphate; (F) plasmid DNA; and (G) T7 RNA polymerase. The DoE created a cubic IV-optimal design with 192 experimental runs. The DoE method allowed statistical analysis of variance (ANOVA) whereby a p value less than 0.05 was taken as a significant result.

Product Analysis

The fluorescent signal from eYFP was quantified using a Synergy HT Multi-Mode Microplate Reader (Biotek, Bad Friedrichshall, Germany) with 485/20 nm excitation and 528/20 nm emission filters. The quantity of eYFP was determined by generating a standard curve based on different concentrations of eYFP in BYL translation reactions without a DNA template. The eYFP standard was produced using an in-house in vitro translation system based on *E. coli* (Zawada, 2012) and purified by immobilized metal-affinity chromatography (IMAC) and size-exclusion chromatography (SEC). The concentration of purified eYFP was determined using a colorimetric assay (Bradford, 1976). Firefly luciferase activity was measured with the Luciferase Assay System (Promega) and a GENios Pro microplate reader (Tecan, Mainz-Kastel, Germany). Firefly luciferase purchased from Roche Diagnostics was used as a standard. GOx activity was determined with an assay based on 2,2′-azino-bis(3-ethylbenzothiazoline-6-sulphonic acid) (ABTS) and horseradish peroxidase (HRP) (Sun et al., 2002; Zhu et al., 2006). 2 μL of the cell-free reaction samples were transferred to a 96-well flat-bottom microplate (Greiner Bio-One) and 200 μL assay mix was added into each well resulting in the following final concentrations: 330 mM D-glucose, 3.3 mM ABTS, and 0.25 U HRP in acetate buffer (100 mM, pH 5.5). Activity was measured by change in absorbance at 405 nm at ambient temperature using a Synergy HT Multi-Mode Microplate Reader (Biotek).

Residue-Specific Labeling of Target Proteins

In order to label target proteins fluorescently in an amino acid selective manner the FluoroTect™ $Green_{Lys}$ in vitro Translation Labeling System (Promega) was used according to the manufacturer's instructions. The product contains a modified charged lysine tRNA labeled with the fluorophore BODIPY®-FL. Using this system, fluorescently labeled lysine residues are incorporated into nascent proteins at multiple sites during translation.

Deglycosylation Assay, SDS-PAGE and Immunoblot

The glycosylation of glucose oxidase (GOx) was determined by treatment with PNGase F (NEB, Frankfurt, Germany) and subsequent analysis of the protein molecular weight by SDS-PAGE followed by immunoblotting. SDS-PAGE was carried out using precast NuPAGE 4–12% (w/v) polyacrylamide Bis-Tris gels (Life Technologies, Carlsbad, CA) followed by staining with Coomassie Brilliant Blue R-250. The PageRuler Prestained Protein Ladder (Thermo Scientific, Waltham, MA) was used as a molecular weight marker. The proteins were transferred to a membrane using a BioRad protein transfer apparatus according to the manufacturer's instructions and the membrane was blocked in 5% (w/v) skimmed milk in phosphate-buffered saline (PBS) for 1 h at room temperature. His_6-tagged proteins were detected in a sandwich reaction using 0.2 μg/mL rabbit anti-polyhistidine antibody (Genscript, Piscataway, NJ) followed by incubation with 0.12 μg/mL alkaline phosphatase-conjugated goat anti-rabbit IgG secondary antibody (Jackson ImmunoResearch, Suffolk, UK) and staining with NBT/BCIP (Applichem, Darmstadt, Germany). The membrane was washed with PBS containing 0.05% (v/v) Tween-20 (PBST) between incubations.

Quantification of Functional Full-Size Antibody M12

The human vitronectin-specific full-size antibody M12 was quantified by indirect ELISA (Kirchhoff et al., 2012). High-binding 96-well plates (Greiner Bio-One) were coated with 0.5 μg/mL human vitronectin (R&D Systems, Minneapolis, MN) in PBS for 2 h at room temperature. After blocking with 1% (w/v) BSA in PBS and washing with PBST, the plates were incubated with standard M12 dilutions produced by transient expression in *Nicotiana benthamiana* (kindly provided by Dr. Nicole Raven) and experimental samples of BYL. The plates were then incubated with the secondary antibody, 0.2 μg/mL alkaline phosphatase-labeled goat anti-human lambda LC (Sigma-Aldrich), and the signal was detected by incubating with substrate pNPP (Sigma-Aldrich) and reading the absorbance at 405 nm after 30 min.

Results

Optimizing the Lysate Preparation

The original protocol for the preparation of BYL (Buntru et al., 2014) was optimized for the coupled transcription and translation system by introducing changes to increase the yield and reduce the manufacturing time. The pectinase concentrate Rohament PL was omitted during the preparation of BY-2 protoplasts because it did not affect the preparation time. The concentration of Rohapect UF, which contains pectinases and arabinases, was instead increased from 0.1 to 0.2%, reducing the time required for protoplast generation. The time needed to disrupt the evacuolated protoplasts was also reduced by replacing the nitrogen decompression chamber with a Dounce homogenizer. It was possible to disrupt the protoplasts in a few minutes using 15 strokes of the homogenizer compared to the 30 min incubation period required in the nitrogen chamber. This optimized protocol allowed the preparation of up to 100 mL of BYL from 4 L of BY-2 cell suspension culture with a final protein concentration of 12.9 ± 0.4 mg/mL, which corresponds to approximately 50% of the protein concentration described for cell-free systems based on yeast (Hodgman and Jewett, 2013) and *E. coli* (Shin and Noireaux, 2010).

Optimizing the CFPS Reaction Conditions

The versatility of the original uncoupled BYL system (Buntru et al., 2014) was improved by developing a coupled transcription–translation system that was also cap-independent, which involved the inclusion of extra components (CTP, UTP and T7 RNA polymerase) and the exclusion of the cap analogs present in the original reaction mixture. The magnesium acetate and potassium acetate were replaced with corresponding glutamates, which were shown to be more efficient in cell-free systems based on *E. coli* and yeast (Hodgman and Jewett, 2013; Jewett and Swartz, 2004). The pIVEX_GAA_Omega_Strep-eYFP vector was used as a template.

Many of the above factors are interdependent (Jewett and Swartz, 2004). We used a DoE approach to optimize the system, but first we reduced the number of factors by investigating them individually and eliminating those with unwanted effects. These preliminary experiments showed that amino acids had no impact on the expression of eYFP whereas DTT and spermine had a clear negative effect with increasing concentration (Fig. 1). The lowest tested concentration of creatine kinase (50 μg/mL) achieved the highest eYFP yield and even without any creatine kinase the BYL system still achieved 60% of the maximum efficiency. The DoE runs were therefore carried out in the absence of amino acids, DTT and spermine, and in the presence of 50 μg/mL creatine kinase.

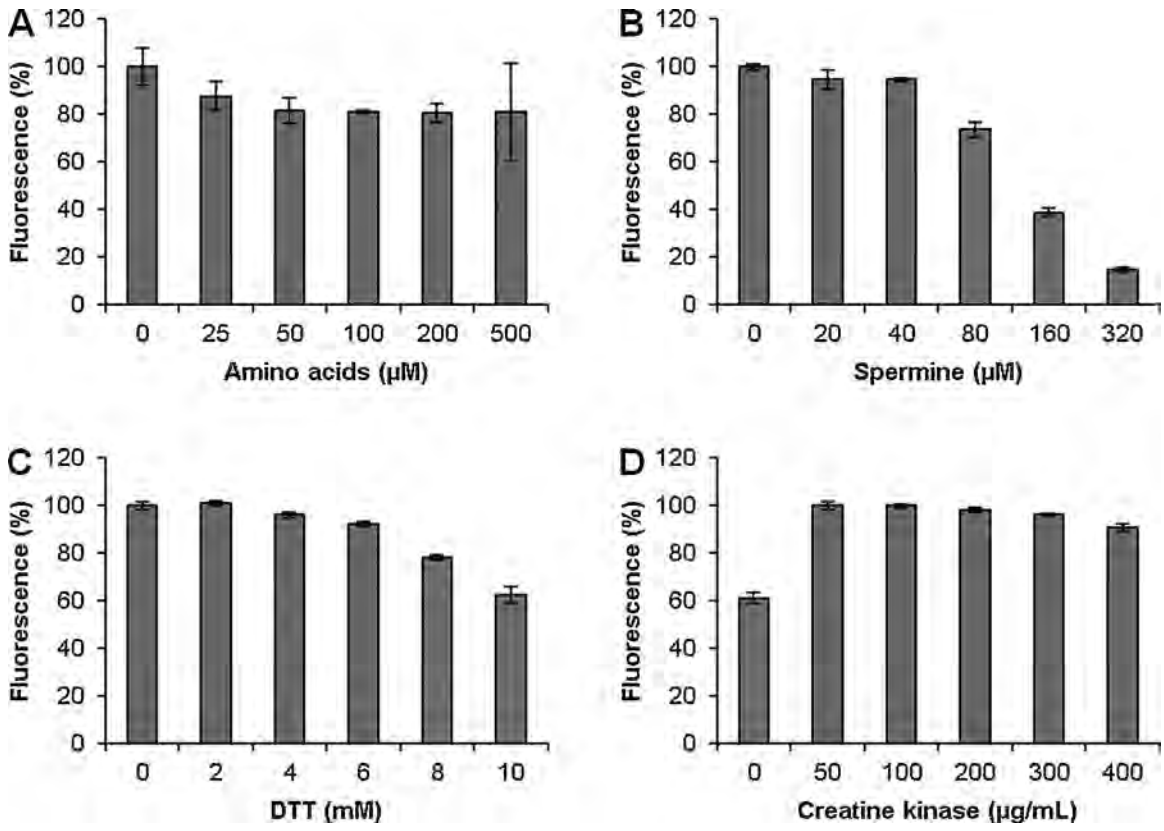

Figure 1. Effect of different concentrations of (**A**) amino acids, (**B**) spermine, (**C**) DTT and (**D**) creatine kinase on eYFP expression in the coupled BYL system. Transcription–translation reactions were carried out using plasmid pIVEX_GAA_Omega_Strep-eYFP as the template at 25°C and 700 rpm for 18 h. Data are shown as relative fluorescence intensities. Control reactions lacking the tested component were set at 100%, except for (**D**) where the lowest tested concentration of creatine kinase (50 μg/mL) was set at 100%. Data represent the averages and standard deviations of three independent transcription–translation experiments.

Table I. Low and high concentration levels of factors screened in the experimental design.

Numeric factor	Factor name	Screened levels
A	HEPES-KOH, pH7.8	0–60 mM
B	Magnesium glutamate	6–14 mM
C	ATP/(GTP/CTP/UTP)	1/0.4–4/1.6 mM
D	Creatine phosphate	15–60 mM
E	Plasmid	20–100 ng/μL (9–43 nM)
F	T7 polymerase	25–100 ng/μL
G	Potassium glutamate	0–80 mM

Table II. Optimal concentrations of reaction components in the coupled BYL system.

Component	Optimum concentration
HEPES-KOH, pH7.8	40 mM
Magnesium glutamate	8.5 mM
ATP/(GTP/CTP/UTP)	3/1.2 mM
Creatine phosphate	30 mM
Plasmid	80 ng/μL (∼34 nM)
T7 polymerase	50 ng/μL
Potassium glutamate	0 mM
Creatine kinase	50 μg/mL

The seven factors selected for testing were the HEPES-KOH buffer (pH 7.8), magnesium glutamate, potassium glutamate, NTPs, creatine phosphate, T7 RNA polymerase and plasmid DNA. These were screened for optimal concentrations using a cubic IV-optimal design with 192 runs. Table I shows the concentration ranges for each of the screened factors. Response surface models were used to predict the factor values required for the optimal target response, i.e., yield (Zhou et al., 2010). A cubic model was fitted onto the experimental data. All non-significant terms ($P > 0.05$ by ANOVA) were dropped. The ANOVA table (Table S2) showed that the model was significant ($P < 0.0001$). The fitness of the model was also confirmed by the multiple R^2 and adjusted R^2 values (0.971 and 0.952, respectively). Strong interactions were observed among magnesium glutamate, NTPs and creatine phosphate (Fig. 2). As expected, higher quantities of NTPs and creatine phosphate, respectively, required a higher concentration of magnesium glutamate. Optimal concentrations of all the reaction components in the coupled BYL system are summarized in Table II, disregarding the amounts already present in the lysate.

Productivity of the BYL Transcription–Translation System

The productivity of the optimized BYL system was tested using a range of model proteins. The production of eYFP was investigated by time course analysis covering the first 20 h of incubation, using pIVEX_GAA_Omega_Strep-eYFP as the template (Fig. 3A). After a lag phase of 2 h, we recorded a linear increase in fluorescence intensity for ∼12 h. The maximum yield (∼200 μg/mL eYFP) was reached after 18 h, and longer reaction times did not achieve any further improvement. Importantly, there was little variation in eYFP yields between different lysate preparations as shown by the average variance of 10% when testing five different BYL preparations in quadruplicate (Table S3).

The productivity of the coupled BYL system was compared to a commercially available coupled WGE system. The four target proteins Strep-eYFP, His-eYFP, eYFP-His, and FFLuc-His were expressed in the BYL using the pIVEX_GAA_Omega construct. Similarly the proteins were expressed in WGE in conjunction with vector pF3A_WG, which was designed specifically for use with this system. For all tested proteins the BYL showed a considerably

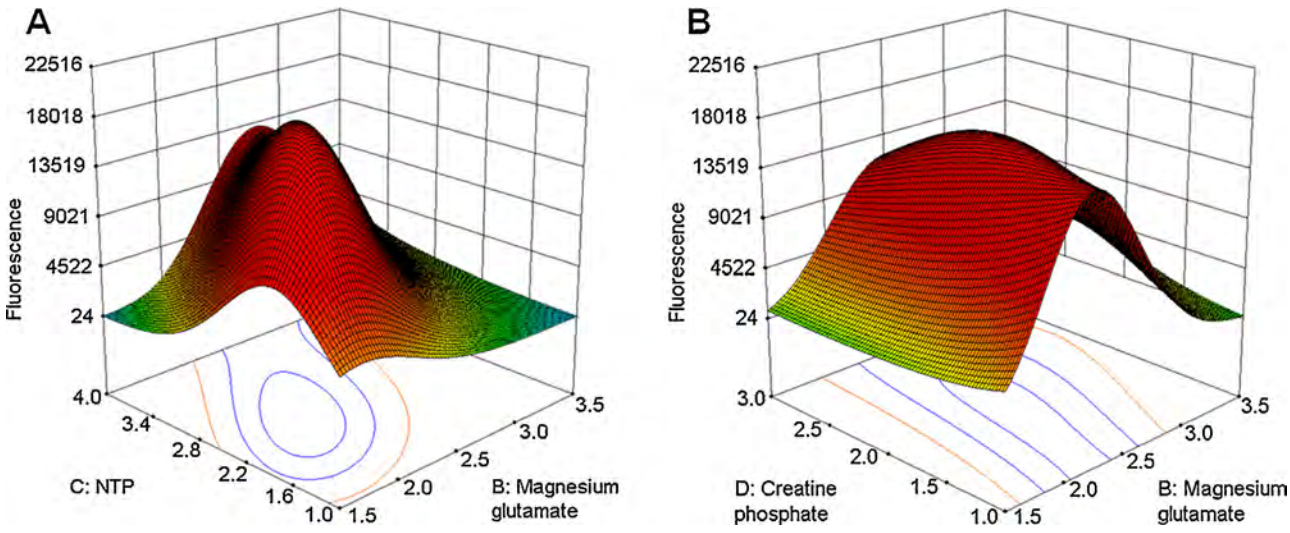

Figure 2. Response surface and contour plots for eYFP synthesis in the coupled BYL system. The effect of two factors on the yield is shown while the other factors are maintained at the determined optimal concentrations. (**A**) Significant interaction between magnesium glutamate and NTP. (**B**) Significant interaction between magnesium glutamate and creatine phosphate.

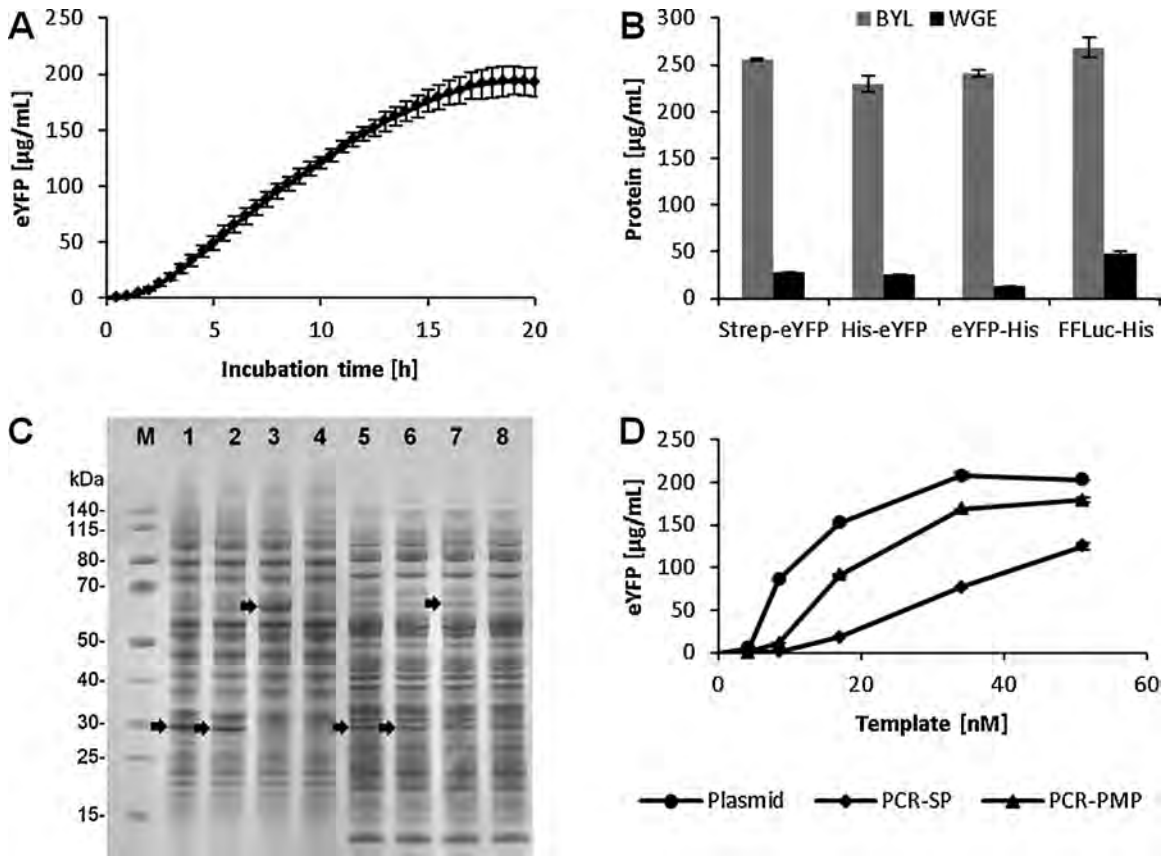

Figure 3. Productivity of the coupled BYL system. (**A**) Time course analysis of eYFP produced by the coupled BYL system over a 20 h run. (**B**) Comparison of the productivities of the coupled BYL system and a commercially available coupled WGE system. (**C**) SDS-PAGE analysis of BYL and WGE transcription–translation reactions. In each case 2 μL of the reaction mix was loaded on a 4–12% (w/v) gradient gel. Lane 1: Strep-eYFP (29 kDa) in BYL, lane 2: eYFP-His (28 kDa) in BYL, lane 3: FFLuc-His (63 kDa) in BYL, lane 4: no template control in BYL, lane 5: Strep-eYFP in WGE, lane 6: eYFP-His in WGE, lane 7: FFLuc-His in WGE, lane 8: no template control in WGE. (**D**) Comparison of CFPS efficiency using different amounts of plasmid and linear templates, the latter produced by PCR using standard (PCR-SP) or phosphorothioate modified (PCR-PMP) primers. All experiments were performed in triplicate.

higher yield than WGE reaching a maximum of target protein for FFLuc-His with 269 ± 10 μg/mL in BYL and 47 ± 3 μg/mL in WGE (Fig. 3B). The higher yield of Strep-eYFP (256 ± 2 μg/mL) compared to the previous experiment can be explained by photobleaching effects during generation of the time course. The coupled BYL system is highly oxygen dependent. Sealing of the transcription–translation reactions using a plastic film reduced target protein yield by almost 90% (Fig. S1).

We used SDS-PAGE to compare 2 μL of the BYL and WGE standard reactions expressing Strep-eYFP, eYFP-His, and FFLuc-His (Fig. 3C). In the BYL system, the additional 29 kDa (Strep-eYFP), 28 kDa (eYFP-His), and 63 kDa (FFLuc-His) bands were easily identified among the endogenous BY-2 cell proteins, whereas in the WGE system endogenous proteins comigrated with these three target proteins .

Vector construction often requires laborious cloning and transformation steps, so we also tested PCR products as templates in the coupled BYL system. We amplified the expression cassette including the T7 promoter, the modified TMV 5′UTR (GAA_Omega), the Strep-eYFP gene, and the TMV 3′UTR from pIVEX_GAA_Omega_Strep-eYFP using standard primers. When 51 nM of the PCR template was included in the BYL reaction, we achieved a Strep-eYFP yield of 125 μg/mL (PCR-SP in Fig. 3D), corresponding to ∼60% of the yield obtained from the plasmid template. However, the plasmid significantly outperformed the PCR product at lower template concentrations. Assuming this reflected the lower stability of the PCR product, we used phosphorothioate-modified primers (PMP) to generate corresponding PCR products that were resistant to cellular exonucleases. The modified PCR product was more stable against degradation in the BYL system (Fig. S2) and achieved a yield of nearly 180 μg/mL Strep-eYFP, representing about 90% of the yield using a plasmid template (PCR-PMP in Fig. 3D). The improvement was even more significant at lower template concentrations. The use of a modified PCR-PMP product therefore significantly reduces the amount of template required to achieve the same amount of target protein.

Translocation of Target Proteins into Endogenous Microsomes

The preparation of the BYL involves the disruption of organelles, but parts of the endoplasmic reticulum (ER) reform as small

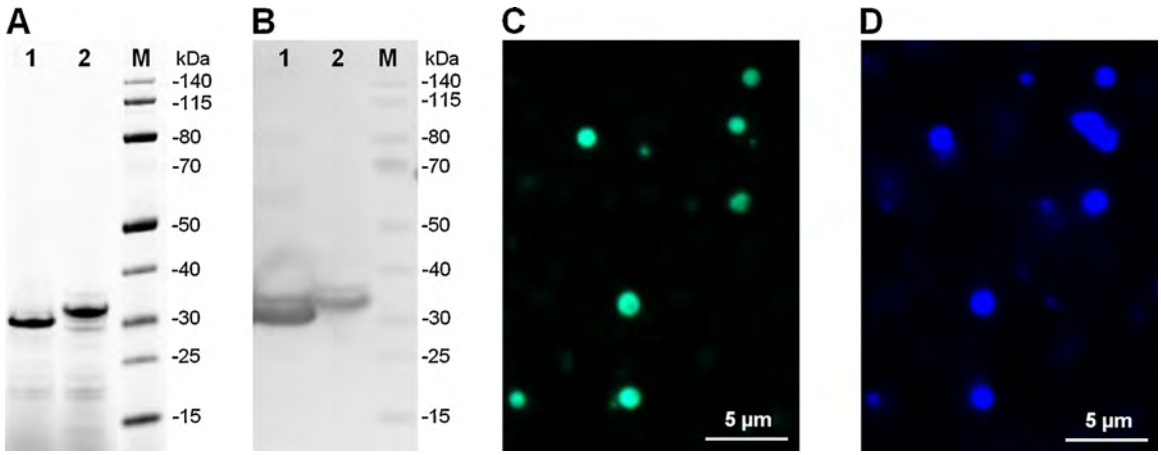

Figure 4. Translocation of MSP-eYFP-His into endogenous microsomes in the coupled BYL system. The target proteins eYFP-His and MSP-eYFP-His were visualized by fluorography and immunoblotting after separation by electrophoresis in a 4–12% (w/v) gradient gel. (**A**) Fluorogram of (1) eYFP-His and (2) MSP-eYFP-His labeled using the FluoroTect™ system (Promega). (**B**) Detection of (1) eYFP-His and (2) MSP-eYFP-His by immunoblot using a rabbit anti-His primary antibody (0.2 µg/mL), a goat anti-rabbit AP-conjugated secondary antibody (0.12 µg/mL) and NBT/BCIP staining. (**C**) Fluorescence analysis of MSP-eYFP-His. Fluorescent vesicles confirm expression and translocation into the lumen of the microsomes. (**D**) Staining of microsomes with ER-Tracker™ Blue-White DPX (Life Technologies) selective for the endoplasmic reticulum.

vesicles known as microsomes. We therefore expressed variants of the eYFP-His protein with and without an N-terminal melittin signal peptide (MSP) to determine whether proteins could be translocated into these organelles. We used two different versions of the pIVEX_GAA_Omega vector to produce the translation products eYFP-His and MSP-eYFP-His, and these were fluorescently labeled by incorporating lysine residues linked to the fluorophore BODIPY®-FL, allowing visualization by fluorography and immunoblotting after separation by SDS-PAGE (Fig. 4A and B). Full-length eYFP-His and MSP-eYFP-His migrated as 29 and 31 kDa bands, respectively, with minimal signs of proteolysis and fragmentation. The translocation of unlabeled MSP-eYFP-His into the microsomes was also confirmed by fluorescence microscopy (Fig. 4C and D). The presence of fluorescent vesicles indicated that MSP-eYFP-His was imported into the lumen of the microsomes. In contrast, eYFP-His lacking a signal peptide was localized externally to the microsomes (data not shown).

Expression of a Type I Transmembrane Protein

We also investigated whether the BYL system could be used to produce integral membrane proteins and target them correctly to microsomal membranes by expressing a type I transmembrane protein, heparin-binding EGF-like growth factor (HbEGF), as an eYFP fusion with an MSP as described above. We used pIVEX_GAA_Omega as the template and MSP-HbEGF-eYFP-His was labeled by incorporating lysine linked to the fluorophore BODIPY®-FL allowing visualization as described above. The full-length MSP-HbEGF-eYFP-His product migrated as a 51 kDa band, again with only minor signs of proteolysis and fragmentation (Fig. 5A and B). Calculated on the basis of eYFP 25 ± 3 µg/mL MSP-HbEGF-eYFP-His was de novo synthesized in the coupled BYL system. Fluorescence microscopy revealed the strong staining of vesicle membranes, confirming the incorporation of MSP-HbEGF-eYFP-His into the microsomal membrane as anticipated (Fig. 5C). Separation of the microsomes by centrifugation showed that around 35% of the produced membrane proteins were integrated into the microsomal membranes (Fig. S3).

Formation of Disulfide Bonds and Glycosylation

The post-translational modification of target proteins was investigated by expressing the model enzyme *Aspergillus niger* glucose oxidase (GOx), which comprises two identical subunits covalently linked by disulfide bonds and contains eight sites for N-linked glycosylation. The protein was expressed using vector pIVEX_GAA_Omega as the template and was targeted to the microsomes using the MSP as described above. Enzymatic activity was compared to a commercial GOx standard using a colorimetric assay with 2,2′-azino-bis-(3-ethylbenzthiazoline-6-sulfonic acid) (ABTS) and horseradish peroxidase (HRP) (Fig. 6B). The MSP-GOx samples had an activity of 2.67 ± 0.02 U/mL whereas GOx without a signal peptide showed only minimal activity (Fig. 6A and B). The cell-free expression of MSP-GOx was also carried out using an eight-fold microsome-enriched lysate concentrated by centrifugation at $5000 \times g$, which is thought to increase the efficiency of translocation and disulfide bond formation. Accordingly, the GOx activity of the microsome-enriched lysate increased to 7.34 ± 0.02 U/mL (Fig. 6C), whereas microsome-depleted BYL showed almost no GOx activity, confirming that translocation into the microsomes is required for correct folding and/or disulfide bond formation.

The MSP-GOx produced by the BYL system yielded two bands, with the more abundant band migrating at 67 kDa and the other at 80 kDa (Fig. 6D). The BYL was mixed with the detergent n-dodecyl-

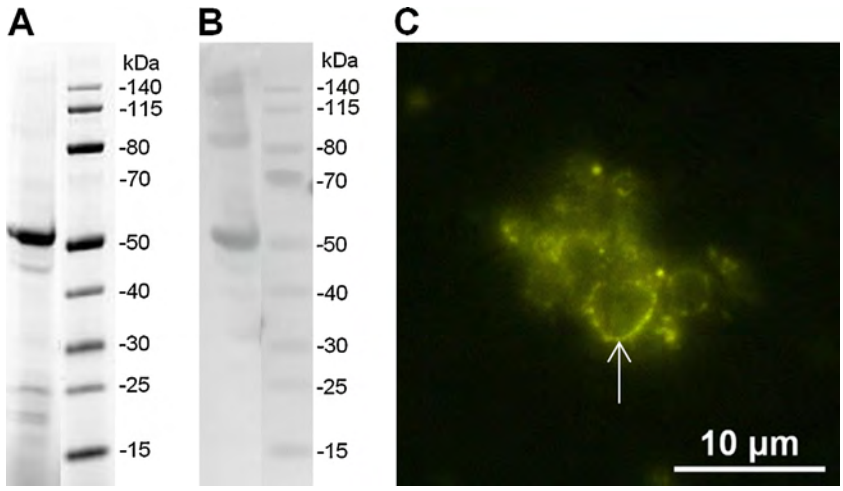

Figure 5. Expression of MSP-Hb-EGF-eYFP in the coupled BYL system. The target protein was visualized by fluorography and immunoblot analysis following separation by electrophoresis in a 4–12% (w/v) gradient gel. (**A**) Fluorogram of MSP-HbEGF-eYFP-His labelled using the FluoroTect^{TM} system (Promega). (**B**) Detection of MSP-HbEGF-eYFP-His by immunoblot using a rabbit anti-His rabbit primary antibody (0.2 µg/mL), a goat anti-rabbit AP-conjugated secondary antibody (0.12 µg/mL) and NBT/BCIP staining. (**C**) Fluorescence analysis of MSP-HbEGF-eYFP-His. Fluorescent membranes indicate the incorporation of the target protein into the microsomal membrane (marked by an arrow).

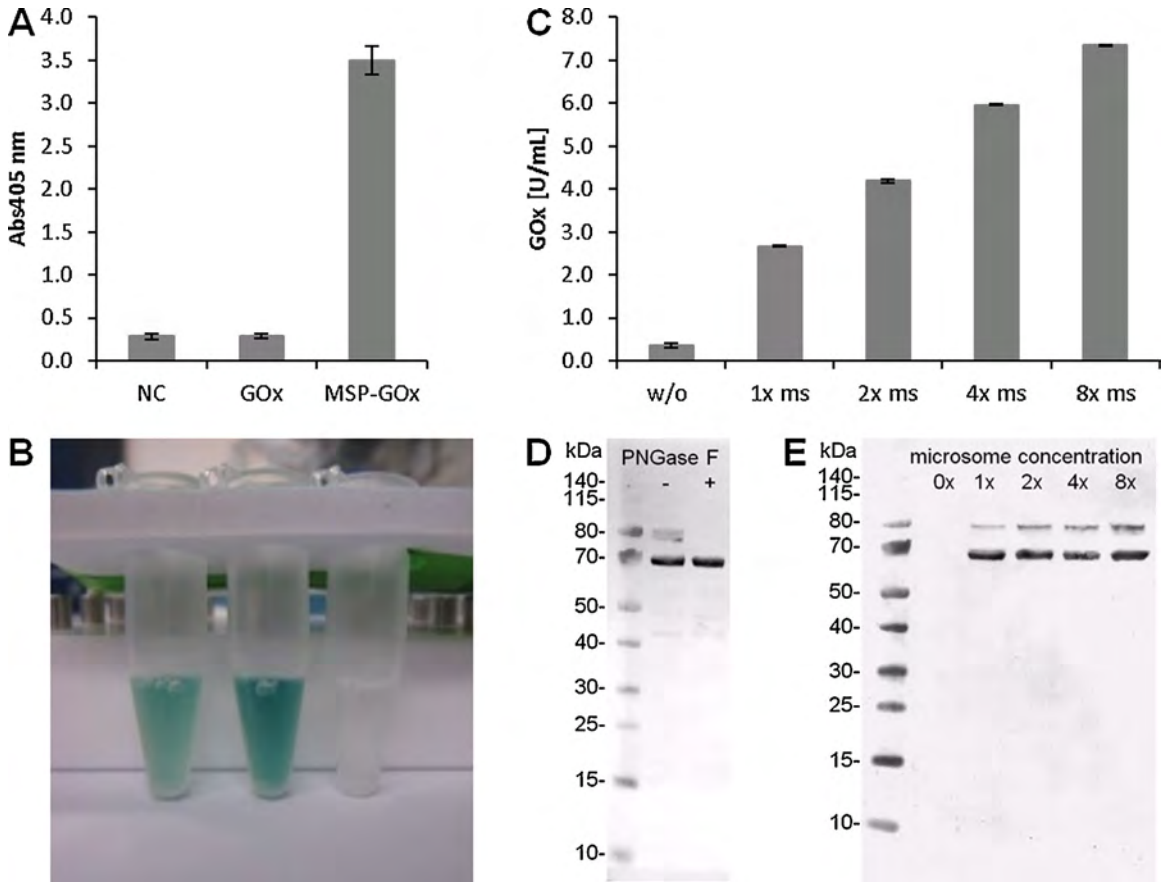

Figure 6. Expression of *Aspergillus niger* glucose oxidase (GOx) in the coupled BYL system. (**A**) Measurement of GOx activity with (MSP-GOx) and without (GOx) an N-terminal melittin signal peptide (MSP) compared to a no-template control (NC). (**B**) Colorimetric assay of GOx activity using ABTS and HRP: (1) 1000 mU/mL GOx standard, (2) MSP-GOx in BYL, (3) no-template control in BYL. (**C**) Measurement of MSP-GOx activity in microsome-enriched BYL. (**D**) Detection of MSP-GOx by immunoblot before (–) and after (+) deglycosylation with PNGase F using a rabbit anti-His primary antibody (0.2 µg/mL), a goat anti-rabbit AP-conjugated secondary antibody (0.12 µg/mL) and NBT/BCIP staining. (**E**) Detection of MSP-GOx expressed at different microsome concentrations by immunoblot using a rabbit anti-His primary antibody and a goat anti-rabbit AP-conjugated secondary antibody.

β-D-maltopyranoside (DDM) to disrupt the vesicular lipid membranes. To confirm that glycosylation was responsible for the observed difference in mass the released protein was digested with PNGase F, which removes almost all types of N-linked glycosylation. Following PNGase F treatment only the 67 kDa band was visible on the gel (Fig. 6D). This confirmed the partial glycosylation of MSP-GOx in the BYL microsomes and the removal of these oligosaccharide groups by PNGase F. The microsome-enriched samples were also analyzed by SDS-PAGE and immunoblotting to determine whether the enhancement of translocation also affected the efficiency of glycosylation (Fig. 6E). Accordingly, we found that the proportion of MSP-GOx represented by the 80 kDa band increased significantly from 12 to 34% (calculated by AIDA) when the enzyme was expressed in the microsome-enriched BYL. A higher amount of microsomes did not increase the overall expression of GOx, but improved the import of the translated protein and thus the formation of active and glycosylated GOx (Fig. S4).

Expression of a Functional Full-size Antibody

The vitronectin-specific full-size human antibody M12 was produced by coexpressing the heavy chain (HC) and light chain (LC) carried by two different pIVEX_GAA_Omega vectors. Both chains were targeted to the microsomes using an N-terminal MSP as discussed above. In the first instance, the chains were expressed in separate transcription–translation reactions, labeled with BODIPY®-FL and visualized by reducing SDS-PAGE as described above. The full-length LC and HC produced bands migrating at 27 and 52 kDa, respectively, with only minor signs of proteolysis and fragmentation (Fig. 7A). Having confirmed the successful expression of each individual chain, they were coexpressed in the coupled BYL system without BODIPY®-FL labelling using different ratios of the LC and HC template plasmids. Samples were separated by non-reducing SDS-PAGE to maintain the integrity of the intermolecular disulfide bonds and the immunoblot was probed with an antibody against the Fc region (Fig. 7B). Typical antibody heterotetramers (~160 kDa) were produced at all the different ratios of LC and HC template plasmids, with the strongest signal achieved at a 1:2 ratio of LC to HC. We also observed HC dimers (~110 kDa), monomers and some degradation products. After DDM treatment to liberate proteins from the microsomes, the concentration of functional M12 antibody was measured against an M12 standard by ELISA using plates coated with human vitronectin. Different dilutions of samples (1:2–1:1024) were incubated in the plates followed by detection using an LC-specific antibody. Samples expressing only the LC or only the HC showed no reactivity because they failed to bind the antigen (data not shown). The coupled BYL system without microsome enrichment yielded 38.5 ± 1.3 μg/mL functional M12 (Fig. 7C), whereas the eight-fold microsome-enriched BYL yielded up to 151.0 ± 20.4 μg/mL, confirming the increased efficiency of protein translocation.

Discussion

We have developed a coupled transcription–translation system based on our previously reported uncoupled BYL system (Buntru et al., 2014) by incorporating the additional components T7 RNA polymerase, CTP and UTP, but removing amino acids, DTT and spermine, which we found to be ineffective or even detrimental (Fig. 1). We also replaced magnesium and potassium acetate with their corresponding glutamates to provide a more authentic representation of the plant cell cytosol, based on similar approaches that led to significant improvements in the cell-free systems based

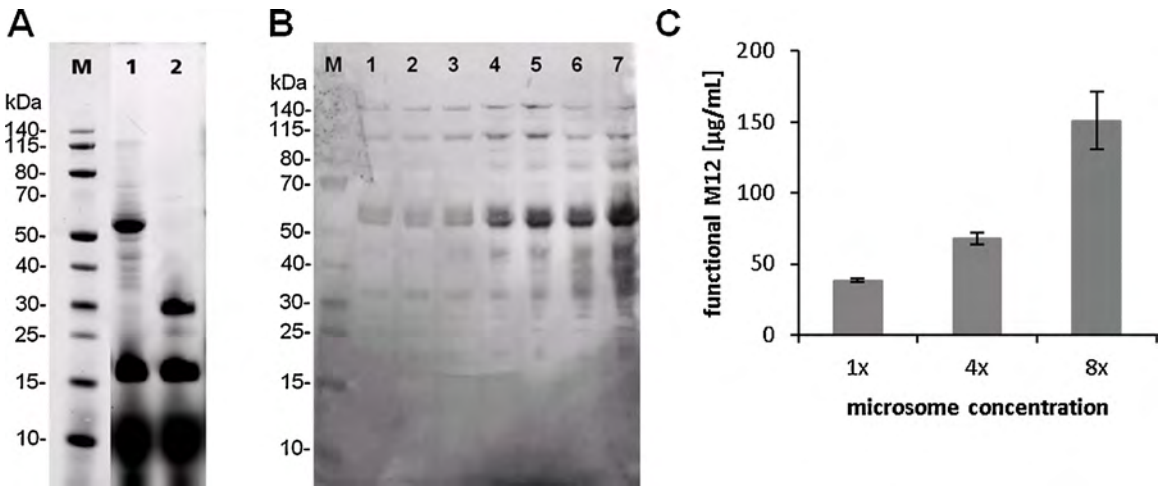

Figure 7. Synthesis of full-size human antibody M12 using the coupled BYL system. (**A**) Fluorogram of the M12 (1) HC and (2) LC labeled with BODIPY®-FL. (**B**) Detection of M12 HC by immunoblot using an AP-conjugated goat anti-human Fc antibody (0.12 μg/mL, Jackson ImmunoResearch) and NBT/BCIP (Applichem) staining. Different ratios of LC to HC template plasmid were used for the coupled transcription–translation reaction: (1) 4:1, (2) 3:1, (3) 2:1, (4) 1:1, (5) 1:2, (6) 1:3, and (7) 1:4. (**C**) The concentration of functional and assembled M12 produced at different microsome concentrations measured by ELISA against human vitronectin, based on a coupled transcription–translation with a 1:2 LC/HC ratio. The concentration was calculated by comparison to M12 standards produced by transient expression in *Nicotiana benthamiana*. Data represent the means and standard deviations of four independent transcription–translation experiments.

on *E. coli* and yeast (Hodgman and Jewett, 2013; Jewett and Swartz, 2004). The costs of the BYL system were reduced by making it cap-independent, thus we removed the cap analog present in the original system and ensured that the expression vectors were equipped with a modified TMV omega sequence (GAA_Omega) that supports cap-independent translation in the WGE system (Sawasaki et al., 2002). The TMV omega sequence was also successfully used in a cap-independent coupled transcription–translation system based on yeast extracts (Gan and Jewett, 2014). The relative concentrations of the reaction components were optimized using a DoE strategy. By a similar approach the target protein yield of a coupled cell-free transcription–translation system based on *E. coli* could be increased by 350% (Caschera et al., 2011). For the BYL the DoE approach resulted in a novel coupled system with the ability to produce a batch yield of up to 270 μg/mL active firefly luciferase within 18 h, which is higher than any other eukaryotic system (Table III).

We also tested linear templates to improve the handling, flexibility and speed of the BYL system for high-throughput applications. Linear templates can be prepared rapidly by PCR avoiding the need for laborious and time-consuming molecular cloning steps. With standard oligonucleotide primers, the resulting PCR products were able to produce up to 125 μg/mL eYFP (Fig. 3D). This is lower than the yields achieved with plasmid templates, presumably reflecting the degradation of linear templates by endogenous exonucleases. We therefore used phosphorothioate-modified oligonucleotides in which three non-binding oxygen atoms at the 5′ end and one at the 3′ end are replaced with sulfur to reduce exonucleases susceptibility (Beaucage and Iyer, 1992; Ciafre et al., 1995; Englisch and Gauss, 1991; Stein et al., 1988; Uhlmann and Peyman, 1990). A similar approach was recently reported in the cell-free *E. coli* system (Sun et al., 2014). The modified PCR products significantly increased the yield of eYFP in the BYL system, especially at lower template concentrations (Fig. 3D). The coupled BYL system is therefore suitable for high-throughput CFPS.

The ability of the BYL system to carry out post-translational modifications was confirmed by the expression of glycosylated GOx, whose activity is dependent on the linkage of two subunits via disulfide bonds (O'Malley and Weaver, 1972). The active glycoprotein was produced successfully if it was targeted to the microsomes, which represent the remnants of the ER and therefore promote the efficient formation of disulfide bonds by providing the correct redox conditions and a flow of oxidizing equivalents from flavoprotein Ero1p via protein disulfide isomerase (Frand and Kaiser, 1999; Tu et al., 2000; Tu and Weissman, 2004). The generation of active GOx suggested that disulfide bonds formed between the correct pairs of cysteine residues, therefore further modifications were not necessary, such as the adjustment of redox conditions using glutathione or the addition of disulfide isomerase as described for insect cell lysates (Merk et al., 2012; Stech et al., 2012), the wheat germ extract (Kawasaki et al., 2003) and the *E. coli* lysate system (Kim and Swartz, 2004; Oh et al., 2006; Yin and Swartz, 2004). The presence of both glycosylated and non-glycosylated GOx was confirmed as described for the expression of human erythropoietin in a cell-free system based on CHO cells (Brodel et al., 2014). However, the microsome-enriched lysates increased the yield of active GOx by 2–3-fold and also increased the proportion of glycosylated GOx (Fig. 6E), similarly reported for the glycosylation of human erythropoietin in the CHO system (Brodel et al., 2014).

Further evidence for the correct assembly of multi-domain proteins containing disulfide bonds was provided by the production of a functional full-size antibody. To our knowledge, this is the first report showing the production of an active, full-size antibody in a eukaryotic cell-free system. Only antibody fragments have been produced thus far in the WGE system (Kawasaki et al., 2003) and in insect cell lysates (Merk et al., 2012; Stech et al., 2012). We achieved a yield of 150 μg/mL for the functional full-size antibody, which is considerably higher than the 20 μg/mL reported for scFv production [Stech et al., 2012] and the 10 μg/mL reported for Fab production (Merk et al., 2012) using insect cell lysates. As described above for GOx, the yield of full-size antibody was increased 4-fold by using microsome-enriched lysates (Fig. 7). Because incompletely formed HC can be prone to aggregation (Ellgaard and Helenius, 2003; Vanhove et al.,

Table III. Batch mode yields and costs of eukaryotic coupled transcription–translation systems.

System	Batch Yield	Costs[h]
Yeast extract	8 μg/mL active firefly luciferase[a]	∼2[a]
Rabbit reticulocyte lysate (RLL)	1–10 μg/mL active firefly luciferase[b]	∼40
Insect cell extract (ICE)	45 μg/mL active firefly luciferase[c]	∼42
Chinese hamster ovary (CHO)	50 μg/mL active firefly luciferase[d]	not available
Wheat germ extract (WGE)	10–100 μg/mL protein[e]	∼43
Leishmania tarentolae extract	220 μg/mL active enhanced green fluorescent protein[f]	∼94
HeLa cell extract	240 μg/mL active firefly luciferase[g]	∼73
BY-2 lysate (BYL)	270 μg/mL active firefly luciferase (this work)	∼0.2

[a](Gan and Jewett, 2014)
[b]Promega TnT® T7 Coupled Reticulocyte Lysate System
[c]Promega TnT® T7 Insect Cell Extract Protein Expression System
[d](Brodel et al., 2014)
[e]Promega TNT® SP6 High-Yield Wheat Germ Protein Expression System
[f]Jena Biosciences LEXSY in vitro Translation Kit
[g]Thermo Scientific 1-Step Human Coupled IVT Kit – DNA
[h]cost of dollar cents per microliter of cell-free reaction

2001), the yield could be increased further by expressing the LC first, allowing it to act as a scaffold for the correct folding and assembly of the HC to form the heterotetrameric full-size antibody.

In conclusion, the coupled BYL system provides a versatile platform for the expression of different classes of proteins including heteromeric, modified and membrane-spanning proteins. With respect to yield and costs the BYL system outperforms all known eukaryotic CFPS platforms (Table III). It is likely that the prolonged activity of the BYL system (nearly 18 h) could be extended even further using a continuous-exchange cell-free (CECF) strategy (Schoborg et al., 2014; Stech et al., 2014). Given that the BYL system can also use PCR products as templates, we now aim to develop a droplet-based microfluidic screening system in our further studies.

We thank Dr. Stefan Kubick (Fraunhofer IZI, Potsdam-Golm, Germany) for vectors pIVEX1.3_eYFP-His, pIX3.0_Strep-eYFP, and pIVEX1.3_MSP-HbEGF-eYFP-His. We also thank Dr. Tanja Holland (Fraunhofer IME, Aachen, Germany) for help with the BY-2 cell cultures, and Dr. Nicole Raven (Fraunhofer IME) for vector pTRAkc_MTAD and the M12 antibody standard. We thank Dr. Raluca Ostafe (RWTH Aachen University, Aachen, Germany) for vector pYES2_GOx. This work was funded by the Federal Ministry of Education and Research (BMBF, FKZ 0315942) and the Fraunhofer Society. Special thanks belong to Dr. Richard M. Twyman (TRM Ltd, York, UK) for the carful revision of the manuscript.

References

Albayrak C, Swartz JR. 2013. Cell-free co-production of an orthogonal transfer RNA activates efficient site-specific non-natural amino acid incorporation. Nucleic Acids Res 41(11):5949–5963.

Beaucage SL, Iyer RP. 1992. Advances in the Synthesis of Oligonucleotides by the Phosphoramidite Approach. Tetrahedron 48(12):2223–2311.

Bradford MM. 1976. A rapid and sensitive method for the quantitation of microgram quantities of protein utilizing the principle of protein-dye binding. Anal Biochem 72:248–254.

Brodel AK, Sonnabend A, Kubick S. 2014. Cell-free protein expression based on extracts from CHO cells. Biotechnol Bioeng 111(1):25–36.

Buntru M, Vogel S, Spiegel H, Schillberg S. 2014. Tobacco BY-2 cell-free lysate: An alternative and highly-productive plant-based in vitro translation system. BMC Biotechnol 14:37.

Carlson ED, Gan R, Hodgman CE, Jewett MC. 2012. Cell-free protein synthesis: Applications come of age. Biotechnol Adv 30(5):1185–1194.

Caschera F, Bedau MA, Buchanan A, Cawse J, de Lucrezia D, Gazzola G, Hanczyc MM, Packard NH. 2011. Coping with complexity: Machine learning optimization of cell-free protein synthesis. Biotechnol Bioeng 108(9):2218–2228.

Caschera F, Noireaux V. 2014. Synthesis of 2.3mg/ml of protein with an all Escherichia coli cell-free transcription-translation system. Biochimie 99:162–168.

Chang HC, Kaiser CM, Hartl FU, Barral JM. 2005. De novo folding of GFP fusion proteins: High efficiency in eukaryotes but not in bacteria. J Mol Biol 353(2):397–409.

Ciafre SA, Rinaldi M, Gasparini P, Seripa D, Bisceglia L, Zelante L, Farace MG, Fazio VM. 1995. Stability and Functional Effectiveness of Phosphorothioate Modified Duplex DNA and Synthetic Mini-Genes. Nucleic Acids Res 23(20):4134–4142.

Czitrom V. 1999. One-factor-at-a-time versus designed experiments. Am Statist 53(2):126–131.

Ellgaard L, Helenius A. 2003. Quality control in the endoplasmic reticulum. Nat Rev Mol Cell Biol 4(3):181–191.

Endo S, Tomimoto Y, Shimizu H, Taniguchi Y, Onizuka T. 2006. Effects of E. coli chaperones on the solubility of human receptors in an in vitro expression system. Mol Biotechnol 33(3):199–209.

Englisch U, Gauss DH. 1991. Chemically Modified Oligonucleotides as Probes and Inhibitors. Angewandte Chemie-International Edition in English 30(6):613–629.

Frand AR, Kaiser CA. 1999. Ero1p oxidizes protein disulfide isomerase in a pathway for disulfide bond formation in the endoplasmic reticulum. Mol Cell 4(4):469–477.

Gan R, Jewett MC. 2014. A combined cell-free transcription-translation system from Saccharomyces cerevisiae for rapid and robust protein synthe. Biotechnol J 9(5):641–651.

Gursinsky T, Schulz B, Behrens SE. 2009. Replication of Tomato bushy stunt virus RNA in a plant in vitro system. Virology 390(2):250–260.

Hodgman CE, Jewett MC. 2013. Optimized extract preparation methods and reaction conditions for improved yeast cell-free protein synthesis. Biotechnol Bioeng 110(10):2643–2654.

Jewett MC, Swartz JR. 2004. Mimicking the Escherichia coli cytoplasmic environment activates long-lived and efficient cell-free protein synthesis. Biotechnol Bioeng 86(1):19–26.

Kawasaki T, Gouda MD, Sawasaki T, Takai K, Endo Y. 2003. Efficient synthesis of a disulfide-containing protein through a batch cell-free system from wheat germ. Eur J Biochem 270(23):4780–4786.

Kim DM, Swartz JR. 2004. Efficient production of a bioactive, multiple disulfide-bonded protein using modified extracts of Escherichia coli. Biotechnol Bioeng 85(2):122–129.

Kirchhoff J, Raven N, Boes A, Roberts JL, Russell S, Treffenfeldt W, Fischer R, Schinkel H, Schiermeyer A, Schillberg S. 2012. Monoclonal tobacco cell lines with enhanced recombinant protein yields can be generated from heterogeneous cell suspension cultures by flow sorting. Plant Biotechnol J 10(8):936–944.

Komoda K, Naito S, Ishikawa M. 2004. Replication of plant RNA virus genomes in a cell-free extract of evacuolated plant protoplasts. Proc Natl Acad Sci U S A 101(7):1863–1873.

Leader B, Baca QJ, Golan DE. 2008. Protein therapeutics: A summary and pharmacological classification. Nat Rev Drug Discov 7(1):21–39.

Matsuda T, Kigawa T, Koshiba S, Inoue M, Aoki M, Yamasaki K, Seki M, Shinozaki K, Yokoyama S. 2006. Cell-free synthesis of zinc-binding proteins. J Struct Funct Genomics 7(2):93–100.

Merk H, Gless C, Maertens B, Gerrits M, Stiege W. 2012. Cell-free synthesis of functional and endotoxin-free antibody Fab fragments by translocation into microsomes. Biotechniques 53(3):153–1560.

Mureev S, Kovtun O, Nguyen UT, Alexandrov K. 2009. Species-independent translational leaders facilitate cell-free expression. Nat Biotechnol 27(8): 747–752.

O'Malley JJ, Weaver JL. 1972. Subunit structure of glucose oxidase from Aspergillus niger. Biochemistry 11(19):3527–3532.

Oh IS, Kim DM, Kim TW, Park CG, Choi CY. 2006. Providing an oxidizing environment for the cell-free expression of disulfide-containing proteins by exhausting the reducing activity of Escherichia coli S30 extract. Biotechnol Prog 22(4):1225–1228.

Ozawa K, Jergic S, Crowther JA, Thompson PR, Wijffels G, Otting G, Dixon NA. 2005. Cell-free protein synthesis in an autoinduction system for NMR studies of protein-protein interactions. J Biomol NMR 32(3):235–241.

Raven N, Rasche S, Kuehn C, Anderlei T, Klöckner W, Schuster F, Henquet M, Bosch D, Büchs J, Fischer R, Schillberg S. 2014. Scaled-up manufacturing of recombinant antibodies produced by plant cells in a 200 L orbitally shaken disposable bioreactor. Biotechnol Bioeng. doi: 10.1002/bit.25352

Sawasaki T, Ogasawara T, Morishita R, Endo Y. 2002. A cell-free protein synthesis system for high-throughput proteomics. Proc Natl Acad Sci U S A 99(23):14652–14657.

Schoborg JA, Hodgman CE, Anderson MJ, Jewett MC. 2014. Substrate replenishment and byproduct removal improve yeast cell-free protein synthesis. Biotechnol J 9(5):630–640.

Schwarz D, Dotsch V, Bernhard F. 2008. Production of membrane proteins using cell-free expression systems. Proteomics 8(19):3933–3946.

Shin J, Noireaux V. 2010. Efficient cell-free expression with the endogenous E. Coli RNA polymerase and sigma factor 70. J Biol Eng 4:8.

Stech M, Merk H, Schenk JA, Stocklein WF, Wustenhagen DA, Micheel B, Duschl C, Bier FF, Kubick S. 2012. Production of functional antibody fragments in a

vesicle-based eukaryotic cell-free translation system. J Biotechnol 164(2):220–231.
Stech M, Quast RB, Sachse R, Schulze C, Wustenhagen DA, Kubick S. 2014. A continuous-exchange cell-free protein synthesis system based on extracts from cultured insect cells. PLoS ONE 9(5):-e96635.
Stein CA, Subasinghe C, Shinozuka K, Cohen JS. 1988. Physicochemical properties of phosphorothioate oligodeoxynucleotides. Nucleic Acids Res 16(8):3209–3221.
Sun L, Bulter T, Alcalde M, Petrounia IP, Arnold FH. 2002. Modification of galactose oxidase to introduce glucose 6-oxidase activity. Chembiochem 3(8):781–783.
Sun ZZ, Yeung E, Hayes CA, Noireaux V, Murray RM. 2014. Linear DNA for rapid prototyping of synthetic biological circuits in an Escherichia coli based TX-TL cell-free system. ACS Synth Biol 3(6):387–397.
Swartz JR. 2012. Transforming Biochemical Engineering with Cell-Free Biology. Aiche Journal 58(1):5–13.
Tu BP, Ho-Schleyer SC, Travers KJ, Weissman JS. 2000. Biochemical basis of oxidative protein folding in the endoplasmic reticulum. Science 290(5496):1571–1574.
Tu BP, Weissman JS. 2004. Oxidative protein folding in eukaryotes: mechanisms and consequences. J Cell Biol 164(3):341–346.
Uhlmann E, Peyman A. 1990. Antisense Oligonucleotides—A New Therapeutic Principle. Chem Rev 90(4):543–584.
Vaidya BK, Mutalik SR, Joshi RM, Nene SN, Kulkarni BD. 2009. Enhanced production of amidase from Rhodococcus erythropolis MTCC 1526 by medium optimisation using a statistical experimental design. J Ind Microbiol Biotechnol 36(5):671–678.
Vanhove M, Usherwood YK, Hendershot LM. 2001. Unassembled Ig heavy chains do not cycle from BiP in vivo but require light chains to trigger their release. Immunity 15(1):105–114.
White ER, Reed TM, Ma Z, Hartman MCT. 2013. Replacing amino acids in translation: Expanding chemical diversity with non-natural variants. Methods 60:70–74.
Wu PS, Ozawa K, Lim SP, Vasudevan SG, Dixon NE, Otting G. 2007a. Cell-free transcription/translation from PCR-amplified DNA for high-throughput NMR studies. Angew Chem Int Ed Engl 46(18):3356–3358.
Wu QL, Chen T, Gan Y, Chen X, Zhao XM. 2007b. Optimization of riboflavin production by recombinant Bacillus subtilis RH44 using statistical designs. Appl Microbiol Biotechnol 76(4):783–794.
Xu Z, Chen H, Yin X, Xu N, Cen P. 2005. High-level expression of soluble human beta-defensin-2 fused with green fluorescent protein in Escherichia coli cell-free system. Appl Biochem Biotechnol 127(1):53–62.
Xun Y, Tremouilhac P, Carraher C, Gelhaus C, Ozawa K, Otting G, Dixon NE, Leippe M, Grotzinger J, Dingley AJ, Kralicek AW. 2009. Cell-free synthesis and combinatorial selective 15N-labeling of the cytotoxic protein amoebapore A from Entamoeba histolytica. Protein Expr Purif 68(1): 22–27.
Yabuki T, Motoda Y, Hanada K, Nunokawa E, Saito M, Seki E, Inoue M, Kigawa T, Yokoyama S. 2007. A robust two-step PCR method of template DNA production for high-throughput cell-free protein synthesis. J Struct Funct Genomics 8(4):173–191.
Yin G, Swartz JR. 2004. Enhancing multiple disulfide bonded protein folding in a cell-free system. Biotechnol Bioeng 86(2):188–195.
Zawada JF. 2012. Preparation and testing of E. coli S30 in vitro transcription translation extracts. Methods Mol Biol 805:31–41.
Zawada JF, Yin G, Steiner AR, Yang J, Naresh A, Roy SM, Gold DS, Heinsohn HG, Murray CJ. 2011. Microscale to manufacturing scale-up of cell-free cytokine production–a new approach for shortening protein production development timelines. Biotechnol Bioeng 108(7):1570–1580.
Zhang K, Kaufman RJ. 2006. Protein folding in the endoplasmic reticulum and the unfolded protein response. Handb Exp Pharmacol 172: 69–91.
Zhou Q, Su JJ, Jiang HX, Huang XQ, Xu YQ. 2010. Optimization of phenazine-1-carboxylic acid production by a gacA/qscR-inactivated Pseudomonas sp M18GQ harboring pME6032Phz using response surface methodology. Applied Microbiology and Biotechnology 86(6):1761–1773.
Zhu Z, Momeu C, Zakhartsev M, Schwaneberg U. 2006. Making glucose oxidase fit for biofuel cell applications by directed protein evolution. Biosens Bioelectron 21(11):2046–2051.

Supporting Information

Additional supporting information may be found in the online version of this article at the publisher's web-site.